Analysis of an electric-propulsion gimballed prop-rotor by CAMRAD II

Chihyun Ahn
Seoul National University
Seoul, Republic of Korea

Minho Hwang
Seoul National University
Seoul, Republic of Korea

HaRyun Choi
Seoul National University
Seoul, Republic of Korea

SangJoon Shin
Seoul National University
Seoul, Republic of Korea

ABSTRACT

This paper presents a rapid conceptual design procedure for a 7,000 lb-class quad-tiltrotor vehicle, focusing on optimizing its aerodynamic design of the rotor blade. By conducting a parametric sweep of the key blade geometric parameters, including bilinear twist, rotor solidity, and taper, the study aims to reduce the vehicle gross weight and enhance performance. The aerodynamic performance of each rotor configuration is analyzed by CAMRAD II, and the results are integrated into the overall vehicle sizing task. The findings indicate a significant improvement in propulsive efficiency, leading to a 4.3% reduction in gross weight and an estimated range improvement of 5.7 nautical miles compared against the baseline configuration. This research will contribute to the ongoing development of efficient electrically-driven rotorcraft design by providing insights into the impact of rotor blade geometry on vehicle performance and weight.

INTRODUCTION

Advanced air mobility (AAM) has been proposed as a solution to mitigate both traffic congestion and air pollution in urban areas (Ref. 1), while addressing the need for on-demand short-haul flight transportation (Ref. 2). In response to that, it is anticipated that AAM aircraft will feature vertical takeoff and landing (VTOL) capability and distributed electric propulsion (DEP), characterized by lower acoustic noise and carbon emission. Since the weight-specific energy capacity of a lithium-ion battery is about 10 times lower compared to aviation gasoline (Ref. 3), this factor imposes an overall weight penalty on the electric propulsion system by dictating the available motor power. Moreover, the use of a DEP system results in distinct requirements on major design parameters and target performance, such as target thrust and disc loading. Therefore, it is necessary to explore the design space thoroughly to identify the feasibility of each (electrically-driven) propulsion configuration.

Among the various electrical VTOL (eVTOL) configurations presented, tiltrotor is regarded to be the most feasible one, owing to its vertical takeoff and landing (VTOL) capability along with high-speed cruise performance. As identified from the recent design effort with optimum speed tilt rotor (OSTR) (Ref. 4), which is a tilting rotor equipped with the rotational speed adjusting optimization technique, an energy-efficient rotor design process will take pivotal role in the eVTOL development.

To deal with that issue, rotor design has been attempted within the various domains. Critchfield and Ning (Ref. 5) performed a blade planform design optimization while modeling a simple equivalent circuit of an eVTOL drive system and integrating it within an overall propulsion design process. Clarke and Botero (Ref. 6) attempted multidisciplinary design optimization for a rotor blade geometry by analyzing the overall sound pressure level. Despite those, previous attempts have shown limitation that those failed to evaluate an impact of the propulsion design upon both the performance and structural weight of eVTOL vehicle.

In an effort to address those limitations, this paper will select a quad-tiltrotor configuration, by demonstrating rapid conceptual design procedure on the three electrically-driven tiltrotor vehicles. In order to determine optimal prop-rotor blade geometry for the quad-tiltrotor vehicle, a rigid-bladed prop-rotor baseline configuration will be devised. Bilinear twist, rotor solidity, and blade linear taper ratio will be selected to perform aerodynamic design sweep of a blade. Flight performance of prop-rotor configuration corresponding to each design cases will be analyzed with comprehensive analytical model of rotorcraft aerodynamics and dynamics (CAMRAD) II (Ref. 7). By providing a single rotor performance analysis result into the quad-tiltrotor vehicle configuration, a relevant influence upon the weight and performance will be investigated in a systematic way, and optimal configuration will be determined.

VEHICLE CONCEPTUAL DESIGN PROCEDURE

Baseline vehicle establishment process

This section outlines the present conceptual design process for tiltrotor UAM vehicle (Fig. 1). The overall geometry of the tiltrotor vehicle configuration will be developed by referring to a NASA reference vehicle (Ref. 8). From the given geometric parameters and corresponding aerodynamic characteristics (Tab. 1), component weight and mission performance of aircraft will be estimated through sizing tasks and trim analysis using NASA Design and Analysis of Rotorcraft (NDARC) (Ref. 9). Low-fidelity aerodynamic analysis codes will be adopted to obtain the aerodynamics of the fuselage and main/auxiliary wings, enabling rapid iterations in the design modification. Through a series of steps, the conceptual design of three electric-driven tiltrotor vehicles with different propulsion configurations (two, four, and six rotors) will be presented, along with their mission performance. Based on this analysis, an optimal configuration will be determined.

Payload weight, design gross weight (DGW) and cruise range requirement will be determined by referring to that of the existing eVTOL vehicle (Refs. 10,11). Design gross weight will be selected to be a nominal value of 7,000 lbs. Based on the Midnight vehicle's five-passenger carrying capacity and assuming a passenger weight of 200 lbs (Ref. 12), the payload weight will be set to 1,000 lbs. Considering the cruise range of the Archer 'Midnight' short-haul flight mission, the one-way flight range for the present mission profile will be set at 17.4 *nmi* (Fig. 2). With a predetermined MTOW of 7,000 lbs, the cruise flight speed of the present mission profile will be adjusted for three baseline configurations to meet the target value (Fig. 3).

The key rotor geometric parameters and nominal operating condition will be determined as follows. Rotors with high disc loading are known to reduce power efficiency during hover (Ref. 13). This can negatively impact the motor's power margin or increase the maximum torque requirement, thus leading to an increase in the weight of the propulsion system, including the thermal management system (Ref. 14). Therefore, by drawing on the existing tiltrotor vehicle trend (Ref. 15) and considering the baseline DGW, the nominal rotor disc loading will be selected to be 10 lb/ft^2. Considering that the hover tip speed of NASA reference vehicle was set to 550 ft/sec to achieve low-noise flight performance, the same specification will be applied to the present vehicle. Because the initial baseline sizing procedure does not involve a detailed design or high-fidelity aerodynamic analysis of the rotor, power and drag performance estimations from the reference vehicle prop-rotor will be adopted. To avoid any substantial deviation in rotor performance while modifying its geometry, solidity-weighted weight coefficient, nominal indicative of the prop-rotor static stall limit, is kept consistent between the reference and present baseline configurations. Referring to the values adopted by large tiltrotor rotary-wing aircraft such as V-22, XV-15, and NASA reference vehicle, a nominal value of 0.13 for the tiltrotor configuration will be assigned. Thus, the rotor solidity and radius are determined for each baseline configuration. Considering that the rotor natural frequency is nominally placed regarding the mission envelope of the rotorcraft (Ref. 16), the first flapwise natural frequency, which is a crucial factor in the weight of the rotor blade, will be selected to be the same as that of NASA reference vehicle owing to the similarity.

The battery-specific energy will be set to reflect the electric battery capacity corresponding to the current technology standards. Accordingly, the uninstalled pack-level battery-specific energy will be set at 250 Wh/kg (Ref. 17).

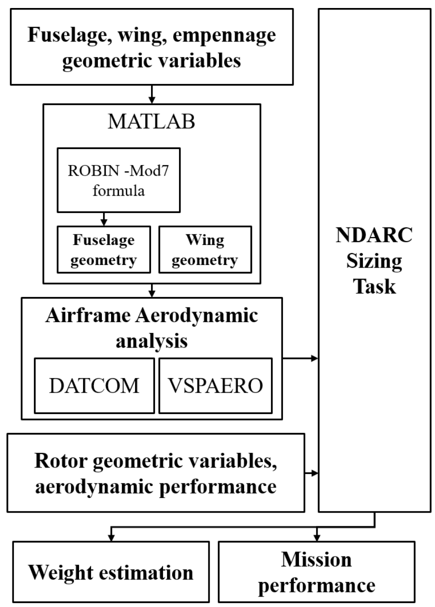

Figure 1. Baseline vehicle establishment procedure

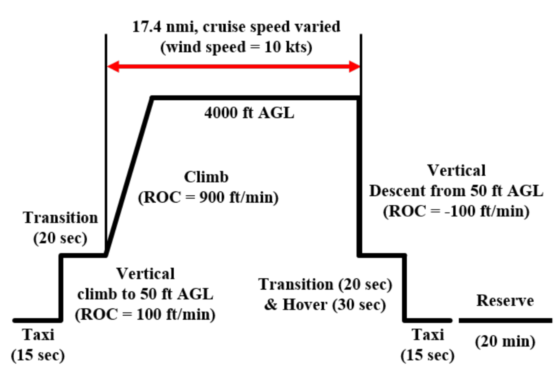

Figure 2. Mission profile for the baseline sizing (1st)

Geometric configuration of fuselage and wings will be generated and its performance will be analyzed as follows. To

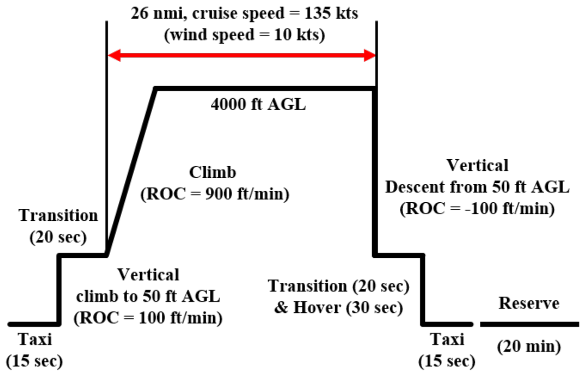

Figure 3. Additional mission profile for performance identification (2nd)

Table 1. Predetermined key design parameters

Parameter	Value
Battery specific energy[a] [Wh/kg]	250
Payload weight [lb]	1,000
Design gross weight	7,000
Solidity-weighted weight coefficient (C_w/σ)	0.13
Disc loading [lb/ft^2]	10
Blade tip speed (hover) [ft/sec]	550
Blade first flapwise natural frequency [/rev]	1.07

[a]Uninstalled pack-level

construct the fuselage geometry in the longitudinal sections, the parameterized NASA ROBIN-mod7 formula will be employed (Ref. 18). Given the NASA reference tiltrotor vehicle transport capacity of six passengers, closely resembling that of the baseline configuration, the fuselage OML for the present baseline emulates that of the reference vehicle. Additionally, to accurately assess propulsion system variations, the fuselage geometry remains consistent across all baselines. The aerodynamic performance of the fuselage will be analyzed by utilizing digital USAF Stability and Control Data Compendium (DATCOM) code, which provides linear aerodynamic load coefficients and stability derivatives of the airframe based on geometric input (including center of gravity) and embedded trend equation (Ref. 19). Wing geometry will be generated with OpenVSP design feature, and its aerodynamic performance will be analyzed with VSPAERO, an aerodynamic analysis code which utilizes vortex-lattice method (Ref. 20). For the present tiltrotor configurations, the wing airfoil will be designated as NACA 64A223, following that of XV-15 tiltrotor vehicle. Referring to the trend of light fixed-wing aircraft and electrically-driven aircraft (Fig.4), the wing planform area will be sized to ensure that the wing loading falls within the range of 25 to 35 lb/ft^2. Overall airframe geometry generation and analysis procedure will be commanded by formatting application programming interface (API) with MATLAB (Ref. 21). The corresponding geometry of each baseline configuration will be generated as shown in Figure 5.

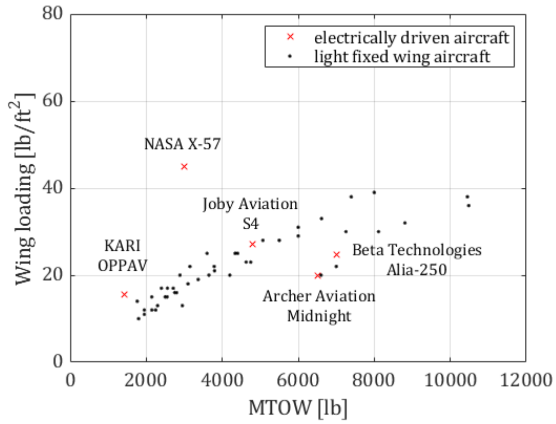

Figure 4. Wing loading of light fixed wing and electrically-driven aircraft

NDARC trim analysis and sizing task will be combined to derive the vehicle configuration that meet the performance requirement (Ref. 9). To effectively obtain a converged trim solution for the performance and geometry of each vehicle, Newton-Raphson method will be employed.

The present trim variables are the vehicle pitch control, longitudinal cyclic, and collective pitch control of rotor, with the nacelle inclination angle selected to be 90° for VTOL segment and 0 ° for forward flight. Since the wing control surfaces are not utilized during cruise for tiltrotor configuration, rotor cyclic pitch control will be introduced to maintain the pitching moment equilibrium of the vehicle. Since the present mission requirement does not include roll or yaw maneuvers, related trim quantities will not be considered. Aerodynamic loads under each trim situation is obtained by using the momentum-theory based rotor performance estimation procedure implemented in NDARC, and aerodynamic performance analysis result of the airframe. With the major control variable estimated respectively for each mission segment, required power for each vehicle component will be obtained accordingly to estimate total energy consumption. Since the battery weight is directly proportional to the energy consumption, subsequent trim iteration over the entire mission with updated battery weight will be attempted until the converged solution is obtained.

At each iteration, the weight of the airframe is estimated by reflecting the aircraft component weight determined at that stage. Wing weight will be estimated by utilizing tiltrotor wing weight trend equation embedded in NDARC (Ref. 9). For the present procedure, torsional and bending moment requirement for the wing will be reflected on structural weight estimation via geometric parameters (span, thickness-to-chord ratio, taper) and wing-tip propulsion system weight. In the similar manner, fuselage weight will be estimated based on AFDD84 trend equation by reflecting overall aircraft specifications, which include fuselage length, aircraft wetted area, rotor radius, wing weight, and crashworthiness condition (Ref. 9). Since detailed structural design will not be conducted during the present conceptual design stage, technical factors representing the airframe structural properties will be determined by following NASA tiltrotor reference vehicle (Ref. 8).

Rotor blade aerodynamic design process

This section presents the aerodynamic design procedure for the electrically-driven prop-rotor blade, as illustrated in Figure 6. To assess the impact of rotor aerodynamic design on weight and performance estimation for the eVTOL tiltrotor configuration, representative blade geometric parameters will be determined. A parametric sweep will then be conducted using aerodynamic analysis with CAMRAD II. In order to determine a rotor blade design that derives minimum gross weight, each blade geometry will be fed back to NDARC tiltrotor vehicle sizing task, along with its aerodynamic performance.

In order to provide airfoil design with benign performance, CTR airfoil series, which is designed for NASA large civil tiltrotor vehicle, will be utilized (Ref. 22). Since the operating Mach number for the blade section spans the transonic regime (Tab. 2), MSES will be utilized owing to its Euler equation solver for the outer flow and an integral boundary layer model (Ref. 23). For the high-AOA post-stall region, a general estimation for the quasi-steady performance of the airfoil will be utilized to extrapolate over the entire AOA range, by using the formula given in Eqs. 1-3 (Ref. 13) (Fig. 7). Resulting performance data will be formatted to provide a general lookup table for prop-rotor aerodynamic analysis using CAMRAD II, which is a comprehensive rotorcraft aeromechanical analysis code (Ref. 7).

$$C_l = 1.175 sin2(\alpha - \alpha_0) \tag{1}$$

$$C_m = -0.5 sin(\alpha - \alpha_0) + 0.11 sin2(\alpha - \alpha_0) \tag{2}$$

$$C_d = 1.135 - 1.05 cos2(\alpha - \alpha_0) \tag{3}$$

Table 2. Blade airfoil nominal operating condition

Airfoil	r/R	Mach No.	Reynolds No.
CTR1544	0.15-0.45	0.1509	7.0×10^5
CTR4475	0.45-0.75	0.3019	1.21×10^5
CTR7500	0.75-0.99	0.4377	1.21×10^6

Referring to the previous gimballed-hub prop-rotor designs and their kinematic constraints, the number of blades will be set to 3. Since the target thrust and disc loading will be fixed at 7000 $lb/(N_{rotor})$ and 10 lb/ft^2, rotor radius will be maintained throughout the entire parameter sweep process. By referring to the previous design research on NASA large civil tiltrotor vehicle (Ref. 24), bilinear twist rate, thrust-weighted rotor solidity (σ_{tw}), and linear taper will be selected. To establish a design space where blade static stall does not occur, a bilinear twist sweep will be performed, followed by solidity and taper sweeps. Following the example of NASA tiltrotor reference vehicle, which operates at lower speeds similar to present tiltrotor vehicles, the blade baseline geometry will be determined to perform a twist sweep; initial values for thrust-weighted solidity and linear taper will be set at 0.141 and 0.8, respectively. Performance analysis for each (rigid-bladed) prop-rotor configuration will be executed by utilizing the blade element momentum theory (BEMT) and uniform inflow model with CAMRAD II. To accurately reflect the influence of aerodynamic performance for each blade section in the rotor performance analysis, 19 aerodynamic panels will be uniformly distributed. The aerodynamic performance of the rotor system will be obtained for designated thrust conditions during hover and cruise segments, the most energy-intensive segments of the mission. Thrust requirement for single rotor at each flight mode will be given based on mission performance analysis result obtained with NDARC trim analysis. To feed the aerodynamic performance of each rotor geometry back to NDARC sizing task, mean section profile drag coefficient (c_{do}) and excess induced loss coefficient (κ_i) will be obtained. In order to assign a benign built-in twist value to the blade that avoids rotor static stall, bilinear twist sweep is performed primarily. After the following solidity & taper sweep, another bilinear twist sweep is performed. Through a series of blade geometry parameter sweeps, the blade configuration that results in the lowest vehicle gross weight will be determined.

VEHICLE CONCEPTUAL DESIGN RESULT

Baseline vehicle design

The initial design of electrically-driven tiltrotor vehicles for three candidates (two, four, and six rotors) is performed. The geometry and performance parameters are fed to NDARC mission performance analysis and weight estimation task. It is noted that the cruise flight velocities of 7,000 lb-class twin-, quad-, hexa-tiltrotor vehicles will be adjusted to 125.2, 123.3, and 116.7 kt, respectively. The resulting design characteristics of the baseline vehicles obtained using the proposed procedure are presented in Tables 3, 4.

With the resulting vehicle geometries, NDARC mission performance analysis result is provided. The energy consumption and total power required at each mission segment are shown in Figs. 8 and 9. As shown in Fig. 8, relative magnitude of the energy consumption remains constant for the vertical and forward flight segments. The energy consumption for cruise flight is estimated to be the highest for the twin-tiltrotor. The main wing of the twin-tiltrotor baseline exhibits the largest aspect ratio among all the wings, and VSPAERO deduces the highest lift-to-drag ratio (L/D) for such a wing. However, considering that the energy consumption of both the quad- and hexa-tiltrotor is estimated to be lower overall, it is concluded that the wing area (or its resultant structural weight) acts dominantly on the cruise energy efficiency of the tiltrotor configuration. In case of the quad-tiltrotor configuration, its energy consumption is estimated to be the largest among all climb segments. It is also found that the energy consumption performance of the quad-tiltrotor configuration for the VTOL and cruise segments is the lowest. This suggests that the energy-consumption performance of the quad-tiltrotor configuration

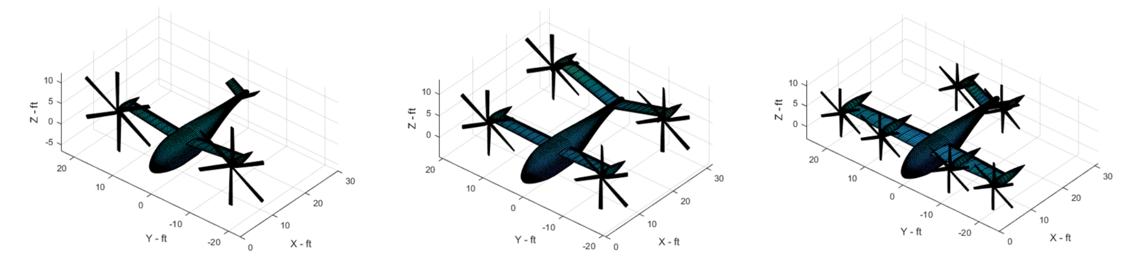

(a) Twin-tiltrotor configuration (b) Quad-tiltrotor configuration (c) Hexa-tiltrotor configuration

Figure 5. Tiltrotor baseline configurations

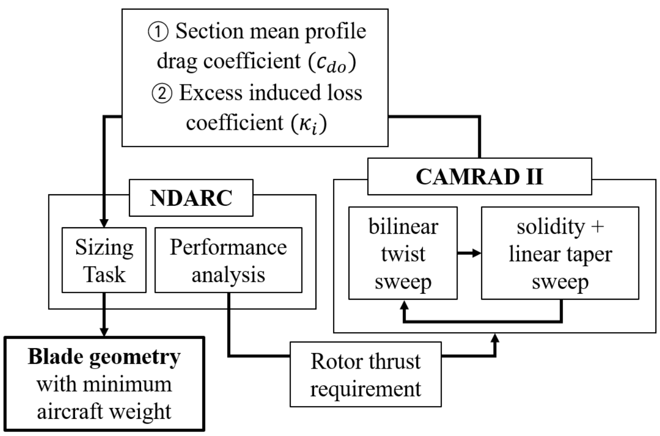

Figure 6. Aerodynamic design procedure for prop-rotor blade

degrades under conditions involving both ascent and forward flight.

Table 3. Geometries of tiltrotor baseline vehicles (7,000-lb class)

Geometry	Characteristics	Twin-	Quad-	Hexa
Fuselage	Length [ft]	30	30	30
	Width [ft]	4.8	4.8	4.8
Wing	Total area [ft^2]	240	220	235
	Span (aft/forward) [ft]	42.2/12.2	28/26.8	32/20
	Wing loading [lb/ft^2]	27.1	31.8	29.8
Rotor	Solidity (σ_{tw})	0.14	0.14	0.14

The required power analysis result is shown in Fig. 9. It is noted that the required power for the hexa-tiltrotor fluctuates heavily with respect to the cruise speed during all the segments. Moreover, required power for the vertical climb and descent segments is estimated to be smaller for the quad- and hexa-tiltrotor configurations than for the twin-tiltrotor configuration. As shown in Fig. 8, overall performance fluctuation turns out to be the smallest for the quad-tiltrotor configuration. This is apparent when compared with the performance of the twin-tiltrotor configuration. Although the speed discrepancy between the twin-tiltrotor and quad-tiltrotor configuration is nearly negligible when switching from the 1st to the 2nd mission, the quad-tiltrotor retained the best performance for all segments in terms of the required power. The twin-tiltrotor exhibits rather inconsistent characteristics, as its energy consumption and required power varies significantly with respect to its cruise speed.

Table 4. Tiltrotor baseline vehicle sizing result (7,000-lb class)

Property	Twin-	Quad-	Hexa-
Empty weight [lb]	5,989	5,989	5,998
Battery&TMS weight [lb]	1,968	1,997	1,966
Wing group weight [lb]	307	327	629
Fuselage group weight [lb]	588	588	582
Rotor group weight [lb]	307	327	300
Rotor radius [ft]	10.2	7.46	5.74

Table 5. Tiltrotor baseline vehicle sizing result (at cruise speed = 135 knot)

Property	Twin-	Quad-	Hexa-
Empty weight [lb]	6,397	6,679	6,983
Battery&TMS weight [lb]	2,248	2,415	2,574
Wing group weight [lb]	711	583	641
Fuselage group weight [lb]	558	628	638
Rotor group weight [lb]	307	369	354
Rotor radius [ft]	10.2	8.13	6.13

Unlike high-speed tiltrotor vehicles such as the XV-15 and V-22, where the power required during cruise is almost on the same scale as during hover (Ref. 25), it has been observed in current eVTOL baselines that the power required during hover is more than three times that needed during cruise. As a result, this significantly higher hover power demand dictates the motor available power rather than the cruise power requirement. Such trend is expected to be due to the characteristics of electric propulsion systems. The increased energy consumption associated with higher cruise range or speed translates directly into significantly increased battery weight (Tab. 5), owing to the lower specific energy of batteries compared to aviation gasoline. This additional weight, in turn, substan-

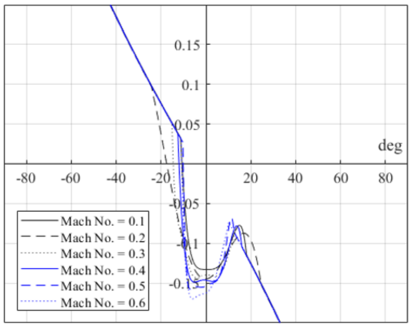

(a) CTR1544 pitching moment analysis result

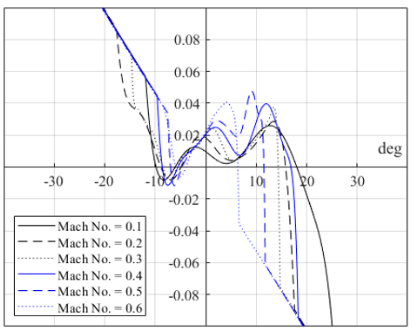

(b) CTR4475 pitching moment analysis result

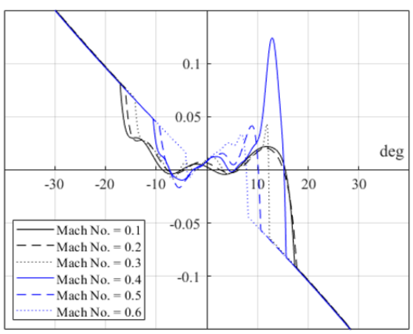

(c) CTR7500 pitching moment analysis result

Figure 7. CTR airfoil pitching moment analysis result

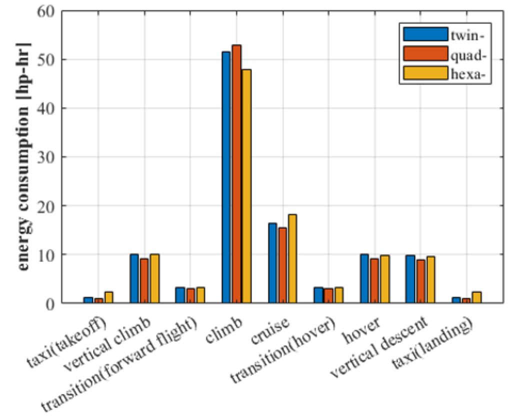

(a) 1st mission profile

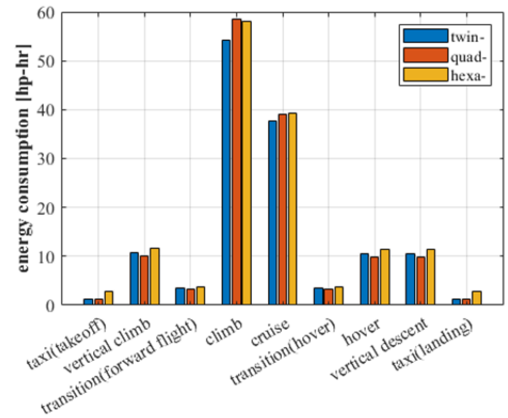

(b) 2nd mission profile

Figure 8. Energy consumption analysis result

tially increases the power required during hover.

Rotor blade aerodynamic design

Present blade design sweep is performed on 7,000 lb-class quad-tiltrotor vehicle, which is determined to be optimal configuration at the initial estimation. Bilinear twist sweep is performed in 5 deg/r step, ranging from -60 deg/r to -10 deg/r. Solidity sweep is conducted from 70% to 120% of the baseline solidity (0.141) in 4% step. Meanwhile, blade taper sweep ranged from 0.1 to 1.0, with steps of 0.05. Optimum blade geometry selected at each step is as summarized in Table 6. NDARC weight estimation results mapped to each parameter sweep case are as depicted in Figs. 10. Aircraft gross weight is estimated to be minimum at blade bilinear twist rate of -55(inboard)/-25(outboard) deg/r. Rotor solidity and blade taper are determined to be 0.1043 and 0.5, respectively. Through the blade geometric parameter sweep, the gross weight of the quad-tiltrotor baseline vehicle is reduced by 297 lb, which accounts for 4.3% of the design gross weight. Applying the corresponding blade design to the sizing of a 7,000 lb-class quad-tiltrotor vehicle resulted in an estimated range increase of approximately 5.7 nmi compared to the baseline configuration.

From the weight estimation results in Figure 10 and Table 6, it is shown that the thrust requirement increases inversely with solidity. Despite the decrease in thrust margin and the consequent reduction in figure of merit, it has been observed that the increase in propulsive efficiency leads to a reduction in cruise energy consumption, resulting in a significant decrease in both battery and aircraft weight. As shown in Figure 10, where the influence of bilinear twist and taper on aircraft weight is not as significant compared to solidity, it is observed that, with the airfoil maximum lift and lift-to-drag ratio fixed, solidity should be adjusted before other geometric parameters to obtain optimal rotor design. Additionally, the solidity must be set considering at least two flight modes, such as hover and cruise.

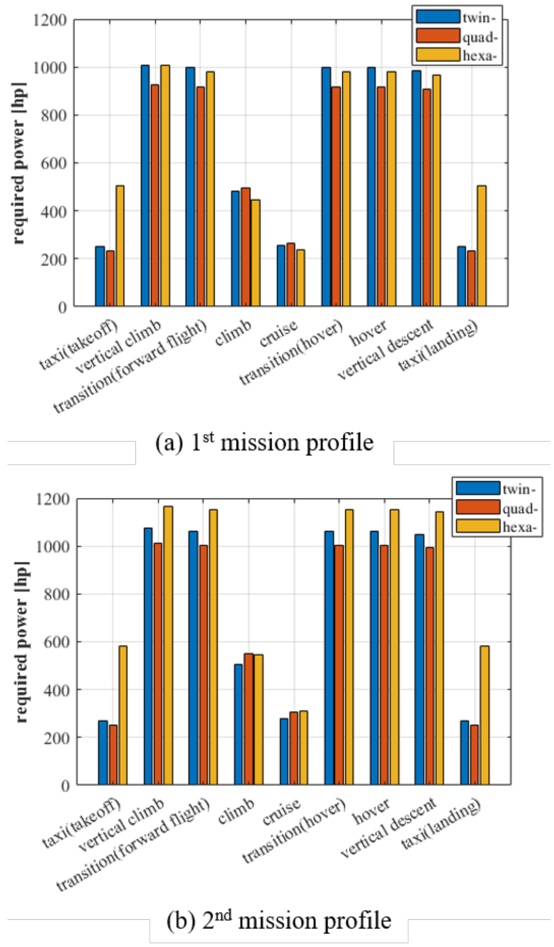

(a) 1st mission profile

(b) 2nd mission profile

Figure 9. Required power analysis result

CONCLUSIONS

In this paper, a rapid conceptual design procedure for a tiltrotor vehicle is presented, augmented by the aerodynamic design of the rotor blade. For that, the following steps are taken. First, the major aircraft design parameters and mission profile are determined by referring to the trends of existing vehi-

Table 6. Blade geometric parametric study history

twist rate(in/out) [deg/r]	-60/-25	-60/-25	-55/-25
built-in twist [deg/r]	-42.5	-42.5	-40
blade linear taper ratio	0.8	0.5	0.5
solidity(σ_{tw})	0.141	0.1043	0.1043
aircraft gross weight [lb]	7,046	6,706	6,704
figure of merit (F_M)	0.749	0.747	0.750
propulsive efficiency (η)	0.872	0.910	0.906
profile drag coefficient (hover)	0.00844	0.01112	0.01106
profile drag coefficient (cruise)	0.00620	0.00644	0.00635
excess induced loss factor (hover)	1.2377	1.2378	1.2377
excess induced loss factor (cruise)	4.5850	3.8844	4.2900
thrust requirement (C_T/σ) (hover)	0.120	0.162	0.162
thrust requirement (C_T/σ) (cruise)	0.021	0.027	0.027

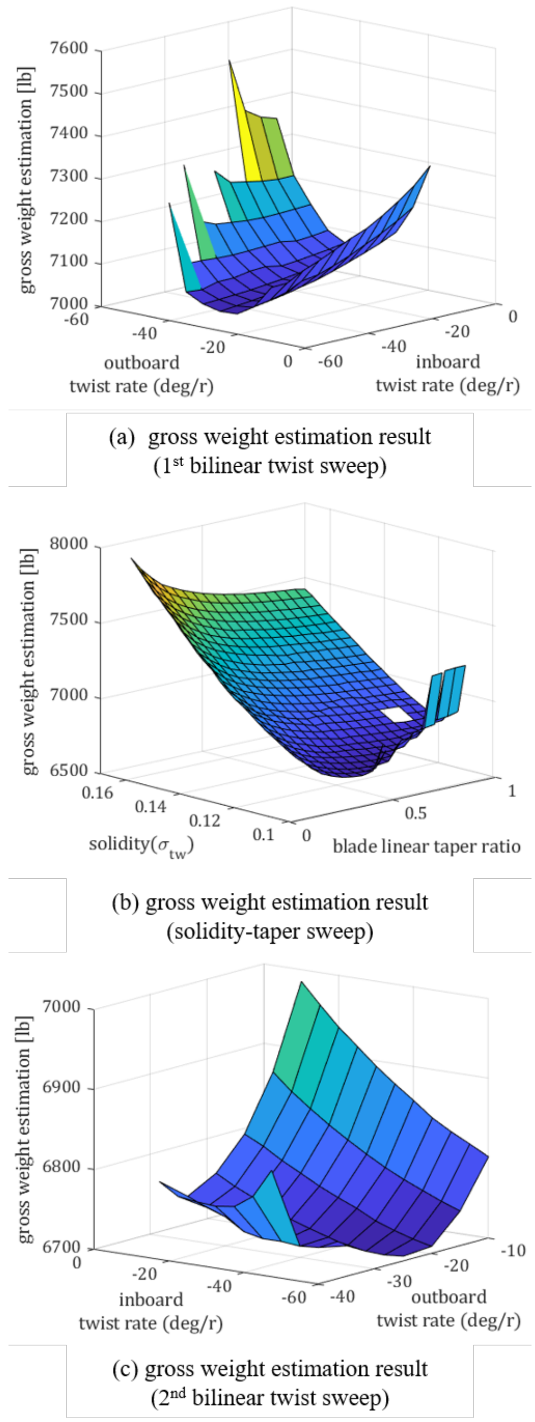

(a) gross weight estimation result (1st bilinear twist sweep)

(b) gross weight estimation result (solidity-taper sweep)

(c) gross weight estimation result (2nd bilinear twist sweep)

Figure 10. Aircraft gross weight estimation result for blade geometry sweep

cles. By conducting aircraft performance analysis and weight estimation, optimal propulsion configuration is selected. By utilizing rapid BEMT analysis, blade geometric parameter sweep is implemented on the quad-tiltrotor vehicle, thus reducing the aircraft gross weight by 4.3%. By incorporating maneuver flight situations such as turns into the current procedure, it is expected that the feasibility of the existing rotor aerodynamic design can be improved, allowing for more accurate aircraft sizing (Ref. 26).

In the future, the aeroelastic (whirl-flutter) stability and structural robustness of the airframe, including the rotor system, will be evaluated to develop an electrically-driven rotorcraft design procedure that ensures safety.

Author contact: Chihyun Ahn dksclgus97@snu.ac.kr, Minho Hwang hmh2989@snu.ac.kr, HaRyun Choi haroonc@snu.ac.kr, SangJoon Shin ssjoon@snu.ac.kr

ACKNOWLEDGMENTS

This work was supported by the National Research Foundation of Korea (NRF) grant funded by the Korea government (MSIT)(No.2021R1A5A1031868).

REFERENCES

1. Choi, J. H., and Park, Y., "Exploring economic feasibility for airport shuttle service of urban air mobility (UAM)," *Transportation Research Part A: Policy and Practice*, Vol. 162, 2022, pp. 267–281. DOI: 10.1016/j.tra.2022.06.004.

2. Antcliff, K., Borer, N., Sartorius, S., Saleh, P., Rose, R., Gariel, M., Oldham, J., Courtin, C., Bradley, M., Roy, S., and Lynch, B., "Regional Air Mobility: Leveraging Our National Investments to Energize the American Travel Experience," NASA, April 2021.

3. Beaureau of Transporation Statistics, "Energy Consumption by Mode of Transportation (metric)," https://www.bts.gov/content/energy-consumption-mode-transportation-0, [Accessed: Aug. 15, 2024]

4. Singh, P., "Flight Dynamics and Control of the Butterfly eVTOL Aircraft in Hover," Vertical Flight Society's 79th Annual Forum & Technology Display, West Palm Beach, FL, May 2023.

5. Critchfield, T. and Ning, A., "Low-fidelity design optimization and parameter sensitivity analysis of tilt-rotor eVTOL electric propulsion systems," Paper AIAA 2023-0325, AIAA SciTech 2023 Forum, National Harbor, MD, Jan. 23–27, 2023.

6. Clarke, A. M. and Botero, E., "Aeroacoustic Optimization of VTOL Rotor Blades," Paper AIAA 2023-0209, AIAA SciTech 2023 Forum, National Harbor, MD, Jan. 23–27, 2023.

7. Johnson, W., "CAMRAD II Comprehensive Analytical Model of Rotorcraft Aerodynamics and Dynamics," Johnson Aeronautics, Palo Alto, CA, 2005.

8. Radotich, M., "Conceptual Design of Tiltrotor Aircraft for Urban Air Mobility," VFS Aeromechanics for Advanced Vertical Flight Technical Meeting, San Jose, CA, Jan. 2022.

9. Johnson, W., "NDARC NASA Design and Analysis of Rotorcraft," NASA/TP-2015-218751, NASA Ames Research Center, Moffett Field, CA, 2015.

10. Archer, "Archer Midnight," https://www.futureflight.aero/aircraft-program/midnight, 2023. [Accessed: Mar. 4, 2024]

11. Air accidents investigation branch, "AAIB-29460," https://assets.publishing.service.gov.uk/media/6632544902f02aa4f31e4143/VA-1X_G-EVTL_06-24.pdf, 2024. [Accessed: Aug. 16, 2024]

12. Bouchard, M., Louvel, N. and Rancourt, D., "An Assessment of the Environmental and Cost Benefits from the Electrification of Light Trainer Aircraft," Paper AIAA 2023-1772, AIAA SciTech 2023 Forum, National Harbor, MD, Jan. 23–27, 2023.

13. Leishman, J. G., *Principles of Helicopter Aerodynamics*, Cambridge University Press, New York, NY, 2000, Chapter 2–7.

14. Zhu, N., Wang, X., Huang, Q., Ding, C., and Wang,J., "Assessment on fire risk of lithium-ion battery packs with different sizes and states of charge by cone calorimeter," *Journal of Themal Analysis and Calorimetry*, Vol. 148, 2023, pp. 6119–6132. DOI: 10.1007/s10973-023-12099-z.

15. Maisel, M. D., Giulianetti, D. J. and Dugan, D. C., "The history of the XV-15 tilt rotor research aircraft: from concept to flight," NASA History Division, Office of Policy and Plans, National Aeronautics and Space Administration, Washington D.C., 2000.

16. Gandhi, F., Pepe, J. and Smith, B., "High Solidity, Low Tip-Speed Rotors for Reduced eVTOL Tonal Noise," Vertical Flight Society's 78th Annual Forum and Technology Display, Fort Worth, TX, May 10–12 2022.

17. Kennedy, R., "EV battery has 50% more energy density than traditional lithiumion, 10-minute charge," https://pv-magazine-usa.com/2023/02/08, 2023. [Accessed: Feb. 18, 2024]

18. Schaeffler, N. W., Allan, B. G., Lienard, C. and LePape, A., "Progress towards Fuselage Drag Reduction via Active Flow Control: A Combined CFD and Experimental Effort," 36th European Rotorcraft Forum, Paris, France, Sept. 7–9, 2010.

19. Williams, J. E. and Vukelich, S. R., "The USAF Stability and Control Digital DATCOM. Volume II. Implementation of Datcom Methods," ADA086558, Mcdonnel Douglas Astronautics Co., Saint Louis, MO, 1979.

20. Kim, J. and Takeshi, T., "OPENVSP based Aerodynamic Design Optimization Tool Building Method and Its Application to Tailless UAV," 33rd Congress of the International Council of the Aeronautical Sciences ICAS, Stockholm, Sweden, Sept. 2022.

21. Hunt, B. R., Lipsman, R. L., and Rosenberg, J. M., "A guide to MATLAB: for beginners and experienced users," Cambridge university press, 2014.

22. Acree, C. W., Martin, P. B., and Romander, E. A., "Impact of Airfoils on Aerodynamic Optimization of Heavy Lift Rotorcraft," The AHS Vertical Lift Vehicle Design Conference, San Francisco, CA, USA, January 2006.

23. Drela, M., "A User's Guide to MSES 3.05," Massachusetts Institute of Technology (MIT), Cambridge, Massachusetts, USA, 2007.

24. Acree, C. W., "Impact of Aerodynamics and Structures Technology on Heavy Lift Tiltrotors," *Journal of the American Helicopter Society*, Vol. 55, (1), January 2010, pp. 12002. DOI: 10.4050/JAHS.55.012002.

25. Johnson, W., Lau, B. H., and Bowles, J. V., "Calculated performance, stability and maneuverability of high-speed tilting-prop-rotor aircraft," NASA-TM-88349, 1986.

26. Yeo, H., Sinsay, J. D., and Acree, C. W., "Selection of Rotor Solidity for Heavy Lift Tiltrotor Design," *Journal of the American Helicopter Society*, Vol. 55, (1), January 2010, pp. 12010. DOI:10.4050/JAHS.55.012010.